Article

Atmospheric and Environmental Impacts of Volcanic Particulates

DURANT, Adam J., BONADONNA, Costanza, HORWELL, Claire J.

DURANT, Adam J., BONADONNA, Costanza, HORWELL, Claire J. Atmospheric and Environmental Impacts of Volcanic Particulates. *Elements*, 2010, vol. 6, no. 4, p. 235-240

DOI : 10.2113/gselements.6.4.235

Atmospheric and Environmental Impacts of Volcanic Particulates

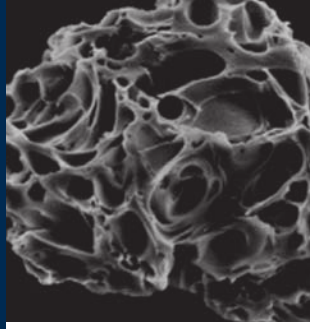

A single ash particle erupted during the 18 May 1980 eruption of Mount St. Helens, USA. The dark voids are vesicles formed as gases escaped. Image width is about 75 µm. USGS IMAGE BY A. SARNA-WOJCICKI

Adam J. Durant[1], Costanza Bonadonna[2], and Claire J. Horwell[3]

1811-5209/10/0006-0235$2.50 DOI: 10.2113/gselements.6.4.235

Volcanic emissions consist of a mixture of gases, aerosol, and silicate particles, which collectively span seven orders of magnitude in size. Airborne ash and sulfate aerosol in the lower atmosphere has short-lived atmospheric and climatic effects. Volcanic aerosol injected high into the stratosphere impacts atmospheric chemical cycles and the solar and terrestrial radiation budgets, and may influence climate over longer timescales than aerosol particles in the lower atmosphere. Once at the surface, the impacts on local environments can be substantial through transport of halogens, trace metals, and metalloids, and subsequent leaching in aqueous solutions. Volcanic emissions may cause disruption to travel and aviation, and may damage surface infrastructure, potentially causing large economic losses.

KEYWORDS: volcanic ash, aerosol, particle, sulfur dioxide, volcano, volcanic cloud, climate, atmosphere

INTRODUCTION

In June 1982, south of Jakarta, Indonesia, a British Airways Boeing 747 flew into a volcanic cloud from an eruption of Galunggung volcano. Airborne volcanic ash abraded the outside of the aircraft, melted as it passed through the jet turbines, and coated internal parts, causing complete loss of thrust. This prompted Captain Eric Moody to announce, while maintaining true British unflappability, "Ladies and Gentlemen, this is your captain speaking. We have a small problem. All four engines have stopped. We are doing our damnedest to get them going again. I trust you are not in too much distress." After descending to within a few hundred meters of the mountaintops on Java, the crew were able to restart all engines and make a safe landing, an incredible feat given the damage to the aircraft and the lack of knowledge regarding how to react in such a situation. The April 2010 eruption of the volcano at Eyjafjallajökull, Iceland, was the most disruptive event in aviation history and caused widespread airport closures due to emissions dispersing through European airspace (see Travelogue this issue). These events, together with several other near-disastrous encounters between commercial airliners and volcanic clouds, emphasize the need for early detection and accurate forecasting of volcanic cloud dispersal patterns.

The atmospheric effects of volcanic emissions have been recognized through historic time. For example, the eruption of Krakatau in 1883 generated fiery sunsets around the Northern Hemisphere, which may have provided inspiration for the alluring backdrop to Edvard Munch's work, *The Scream*. At any moment, at least 20 volcanoes around the globe may be erupting (see www.volcano.si.edu). Collectively these emit a constant flux of gases and particulates into the atmosphere (FIG. 1 AND BOX 1). Volcanoes that are supplied with high-silica magmas tend to erupt more explosively and therefore produce the largest impacts. The first comprehensive effort to quantify the atmospheric effects of volcanic eruptions was made by Lamb (1970), who compiled the Dust Veil Index (DVI) using historical records of atmospheric optical phenomena, and temperature and radiation measurements. Since then, the advent of satellite sensors in space has made it possible to observe and measure the effects of volcanic eruptions in near real-time (Prata 2009) (FIG. 2).

In the following sections we investigate the life cycle and effects of volcanic particulates in the atmosphere, from emission to removal. These effects include short-term influences on microphysical processes and heterogeneous chemical pathways in clouds, transient effects on local environments as particulates settle to the ground, and long-term influences on climate.

EMISSIONS OF VOLCANIC GASES AND PARTICLES

Magma (molten rock) contains a diverse range of dissolved gases, including water vapor, carbon dioxide (CO_2), and sulfur dioxide (SO_2) (Oppenheimer 2010), along with smaller amounts of hydrogen sulfide, hydrogen, helium, carbon monoxide, hydrogen chloride (HCl), hydrogen fluoride, nitrogen, and argon (Grainger and Highwood 2003). Heat generated within the Earth causes magma to rise towards the surface and, as this happens, pressure exerted by the surrounding crustal material decreases. In response, gases come out of solution and form bubbles (vesicles), very much in the same manner as the effervescence that occurs when a container of carbonated drink is opened. Most ash

1 Centre for Atmospheric Science, Department of Chemistry / Department of Geography, University of Cambridge Cambridge, UK; Geological and Mining Engineering and Sciences Michigan Technological University 1400 Townsend Drive, Houghton, MI 49931, USA E-mail: adam.durant@ch.cam.ac.uk

2 Section des Sciences de la Terre et de l'Environnement, Université de Genève, 13 Rue des Maraîchers, CH-1205 Genève, Switzerland

3 Institute of Hazard, Risk and Resilience, Department of Earth Sciences, Durham University, South Road, Durham DH1 3LE UK

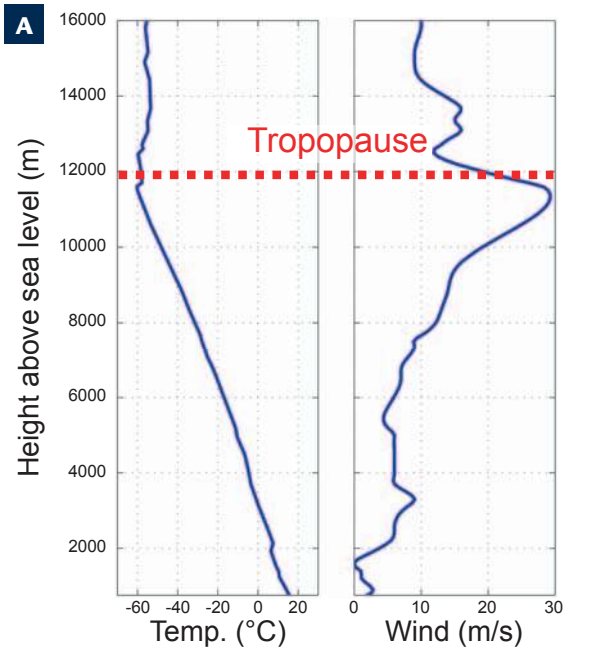

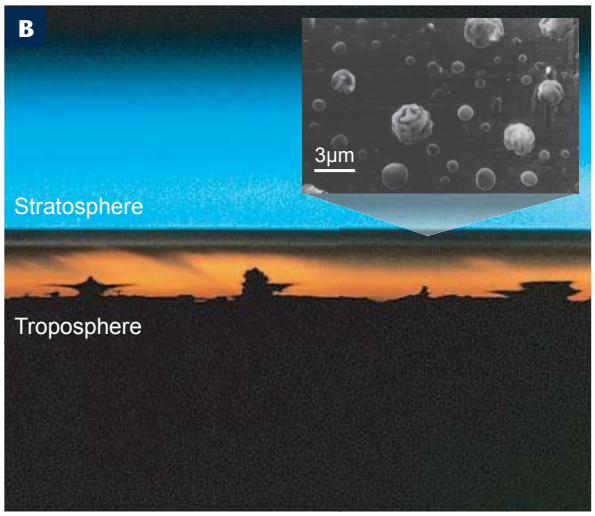

Figure 1 Atmospheric structure and characteristics of volcanic aerosol particles. (**A**) Temperature decreases with height through the troposphere to the tropopause (defined by a temperature inversion). Wind velocity reaches a maximum at the tropopause in the jet stream. (**B**) A veil of stratospheric sulfate aerosol (SSA) from the 1991 eruption of Pinatubo volcano (Philippines) appears as a subtle dark gray layer in the background image. Image Courtesy of NASA. The inset shows long-lived SSA particles (H_2SO_4–H_2O droplets and sulfuric acid–coated volcanic ash) collected by a NASA research aircraft 8 months after the eruption at an altitude of 10.7 km (from Pueschel et al. 1994). Image courtesy of American Geophysical Union

particles are formed through bubble fragmentation when exsolution overpressures are generated in vesicles as magma rises rapidly to the surface (e.g. Sparks 1978).

The flux of volcanic particulates from silicic explosive eruptions is proportional to eruption magnitude (Self 2006; Deligne et al. 2010; Table 1). Specifically, the global annual flux of fine ash (particles < 63 μm) to the atmosphere is estimated at approximately 176–256 Tg (teragrams); i.e. an annual average over 1000 years of 176–256 million metric tons; Table 1). Of this total, tropospheric fluxes of volcanic ash and SO_2 (available to form sulfate aerosol particles) amount to 200 Tg y^{-1} and 5–10 Tg y^{-1}, respectively (Mather et al. 2003). Explosive volcanism contributes approximately 60 wt% of the total global volcanic SO_2 flux, and emissions from a quarter of all eruptions reach the stratosphere (Halmer et al. 2002).

PLUMES, PARTICLES, CLUMPS, AND GRAVITY

The rate at which volcanic particulates settle through the atmosphere to the Earth's surface due to gravity—the terminal velocity (v_t)—is a function of particle size, density (400–3200 kg m^{-3}), and shape. For simplicity, v_t is often calculated assuming a spherical shape, which may provide a realistic approach for sulfate aerosol particles. However, volcanic ash particles have angular and irregular shapes, which generate drag during settling and reduce v_t compared to the v_t of a spherical object. Other factors, such as the atmospheric injection height of the particulates, local wind field, and the initial particle-size distribution, combined with v_t, control the physical characteristics of tephra deposits (e.g. particle size and mass deposited per unit area) as a function of distance from the volcano (see Box 1 for a definition of tephra; Bonadonna et al. 1998).

Table 1 FREQUENCY OF VOLCANIC ERUPTIONS

Magnitude[1]	Total mass (kg)	Mass of fine ash (kg) [2]	Return period (y) [3]	Number of eruptions over 1000 years	1000-year total emission of fine ash (x 10^3 Tg)
4.5	3.2×10^{11}	6.3×10^{10}	4.4	227	14
5.0	1.0×10^{12}	2.0×10^{11}	7.9	127	25
5.5	3.2×10^{12}	6.3×10^{11}	24.0	42	26
6.0	1.0×10^{13}	2.0×10^{12}	49.0	20	41
6.5	3.2×10^{13}	6.3×10^{12}	129.0	8	49
7.0	1.0×10^{14}	2.0×10^{13}	200–1000[4]	1–5	20–100
8.0	1.0×10^{15}	2.0×10^{14}	>120,000[4]	<1	<2

1 Magnitude = $\log_{10}$(erupted mass [kg]) – 7 (Pyle 2000)

2 20% of total mass erupted in silica-rich explosive eruptions is assumed to be fine ash (i.e. particles with diameter < 63 μm) (Mastin et al. 2009).

3 Return period is the rate in years that an eruption of given magnitude will occur based on the Holocene dataset (from Deligne et al. 2010).

4 From Self (2006)

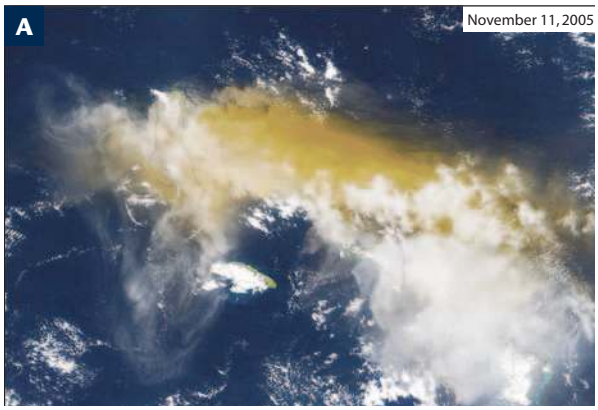

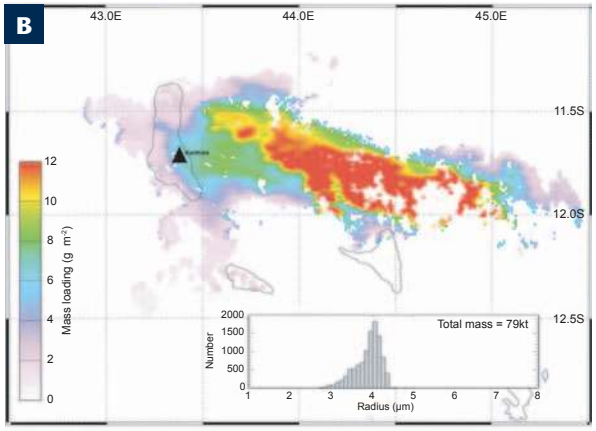

Figure 2 Satellite observations of an eruption of Mount Karthala, Comoros, Indian Ocean (marked by black triangle in B). During dispersion in the atmosphere, ash and SO_2 from the eruption plume separated into discrete layers at different heights, which presented a complex situation for ash-cloud trajectory forecasting and aircraft-hazard mitigation. (**A**) Moderate Resolution Imaging Spectroradiometer (MODIS) visible light image. (**B**) Map of particle characteristics derived from infrared radiation measured at wavelengths of 10 μm and 11 μm, showing cloud particle mass (g/m^2) and, in the inset diagram, the size (radius) distribution of airborne ash particles. Latitudes and longitudes are shown on the margins of B. Modified from an image generated by F. Prata

Tephra may be grouped into four sedimentation categories based on aerodynamic behavior of its components (Bursik et al. 1992). Large centimeter- to meter-sized fragments follow brief (typically <60 s) ballistic trajectories and reach the surface within a few kilometers of the volcano. Smaller particles settle in a time that is a function of v_t and the total distance transported in the vertical and horizontal fields, which depends on the eruption column height.

Figure 3 Weak plume from an eruption of Halema'uma'u vent, Kilauea, Hawai'i (July 2008). Wind velocity exceeds vertical updraft, causing the plume to bend over and rotate, forming a vortex structure. Photo by A. Durant

Millimeter- to centimeter-sized particles (e.g. >16 mm in a 20–30 km high plume) settle from the column within a few minutes and usually land at a distance of less than 15 km from the volcano; particles with diameters ranging from 63 μm to 16 mm are transported to the column top and settle from the high-level spreading cloud within tens of minutes to an hour; particles less than 63 μm in diameter are transported in the dispersing cloud and remain suspended in the atmosphere for hours to days, or longer.

Eruptive plumes with upward velocities lower than wind velocities (i.e. weak plumes) tend to bend over and form pronounced fingering (i.e. convective instabilities) and vortices (Figs. 3, 4A). Tephra deposits from weak plumes are typically elongated in the direction of wind transport; they are characterized by rapid thinning in proximal–medial areas (associated with the bent-over region) and may have multiple accumulation maxima. Emissions from weak, bent-over plumes do not typically penetrate through the tropopause. In contrast, strong plumes rise with typical velocities of 50–200 m s^{-1}, which greatly exceeds local wind velocities, and inject fine ash into the stratosphere within a few minutes to form a horizontally spreading gravity current (Fig. 4B). Fallout from the vertical convective plume (i.e. fallout from the plume margins, <15 km from the vent) is typically poorly sorted, is usually coarser than proximal fallout from weak plumes, and thins exponentially away

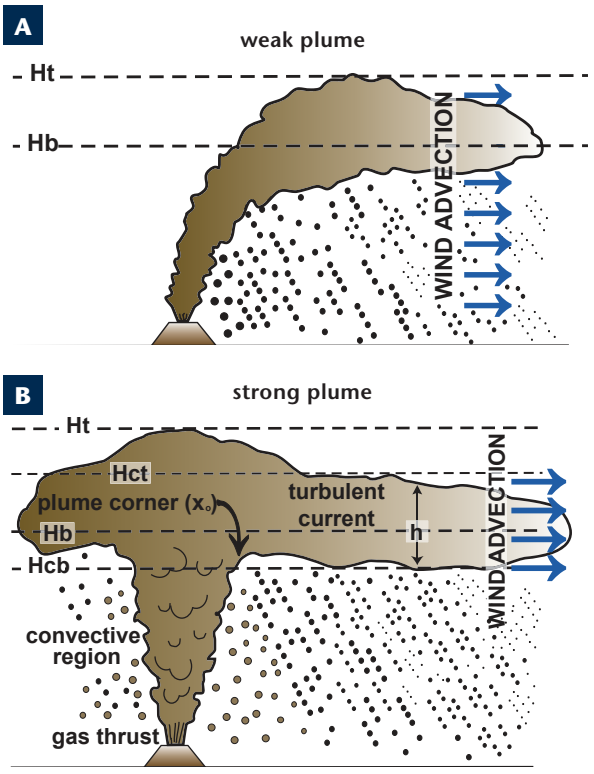

Figure 4 Diagram showing the main features of weak (**A**) and strong (**B**) plumes developing in a wind field, modified from Bonadonna and Phillips (2003). Strong plumes are characterized by a subvertical convective region that spreads laterally around the level of neutral buoyancy, Hb. The total column height, Ht, is controlled by the momentum of the eruptive plume at Hb. Particles are carried in the spreading current with a thickness of h = Hct – Hcb, where Hct and Hcb are the heights of the top and the base of the spreading current, respectively. Particles fall both from the plume margins (brown dots) and from the turbulent current (black dots). Weak plumes have a lower upward velocity than the wind velocity. As a result, they develop into bent-over plumes and start spreading subhorizontally around Hb. Not to scale.

from the source. Fallout from the horizontally spreading current is more widespread than in the case of weak plumes and is characterized by gradual thinning.

The resulting tephra deposits can be elongated downwind when affected by strong winds (e.g. 18 May 1980 Mount St. Helens eruption), or they can be quasi-symmetrical in the absence of wind (e.g. 2450 BP eruption of Pululagua, Ecuador) or when the radial plume velocity is significantly greater than wind velocity (e.g. 15 June 1991 Pinatubo eruption). Tephra deposits from strong plumes may also thicken downwind in response to enhanced accumulation from particle aggregation.

The distal gravitational settling (hundreds of kilometers downwind) of ash particles from both weak and strong plumes almost exclusively involves fine ash. The rate of particle settling may be increased by particle aggregation (related to hydrometeor nucleation and growth, a process that involves the formation of atmospheric particles as a result of water condensation or freezing) and bulk sedimentation from the development of convective instabilities (e.g. mammatus; Fig. 5) (Durant et al. 2009).

A NEW VIEW OF VOLCANIC CLOUDS FROM SPACE

Observed from space, volcanic clouds often have the color and texture of water clouds (Fig. 2A), so detection can be challenging based on visible characteristics alone. The potential for use of meteorological satellites to monitor volcanic clouds was first recognized following the 1982 El Chichón (Mexico) eruption (Krueger et al. 2008). Although the Total Ozone Mapping Spectrometer (TOMS) was designed to measure ozone concentrations in the atmosphere, it was able to detect SO_2 in high concentrations. Meteorological satellite sensors are also capable of detecting the amount and size of ash particles in eruption clouds based on absorption in the thermal infrared [e.g. retrievals using MODerate Resolution Imaging Spectroradiometer (MODIS) imagery, Fig. 2B], and can provide estimates of the height of volcanic emissions in the atmosphere (Prata 2009). Other remote sensing techniques routinely applied include Doppler radar, and ground-based and space-based lidar (laser light detection and ranging), which have the capability to characterize particle size and shape and can identify liquid water and ice particles in the atmosphere.

Figure 5 Pouch-like, lobate mammatus on the underside of the 18 May 1980 Mount St. Helens volcanic cloud over Ephrata, Washington, on the morning of the eruption. Volcanic mammatus have a diameter of ~500 m and contain aggregates of ash and ice. Mammatus are commonly observed on waning-stage thunderstorm anvils. Image Courtesy of D. Miller

IMPACTS ON CLIMATE

For a given eruption, the atmospheric impacts depend on the magnitude (eruption size) and intensity (rate at which emissions enter the atmosphere, which also controls plume height), the location of the volcano, the physical and chemical properties of the emissions, and the residence time of the particles in the atmosphere (which is mainly related to eruption intensity and initial particle-size distribution). Volcanic particulates scatter and absorb solar and terrestrial radiation, and adjust the energy budget of the atmosphere. Long-term (months to years) climatic impacts are caused by volcanogenic stratospheric sulfate aerosol (SSA) (Fig. 1). The effects of tropospheric volcanic aerosol are shorter-lived compared to SSA as precipitation rapidly transports emissions to the surface. Prolonged tropospheric degassing can, however, cause regional impacts on climate and local environments, e.g. the 8-month eruption of Laki volcano, Iceland, in 1783.

High numbers of sulfuric acid (H_2SO_4) aerosol particles with a diameter of <0.02 µm form in the first week after SO_2 injection through photooxidation of SO_2 in the stratosphere and grow over time through coagulation (Box 1). Almost all of the H_2SO_4 produced nucleates on preexisting condensation nuclei and forms liquid H_2SO_4–H_2O particles (the basis of SSA). Evolved SSA includes liquid and solid sulfate particles, which scatter shortwave solar radiation back to space (resulting in a higher planetary albedo), absorb terrestrial longwave radiation, and cause a complex climate response (Robock 2004). For example, the June 1991 eruption of Mount Pinatubo injected ~20 Mt of SO_2 into the stratosphere, and the Northern Hemisphere warmed by up to 3 °C during the 1991–1992 winter and cooled by up to 2 °C in the 1992 summer.

Pyle and Mather (2009) provide an extensive review of volcanic halogen fluxes (fluorine, chlorine, bromine, and iodine) to both the atmosphere and the oceans. Volcanic particulates provide surfaces to catalyze heterogeneous chemical reactions, which can, for example, result in ozone destruction. Ash particles also influence cloud microphysical processes and act as ice-nucleation sites during plume rise (Durant et al. 2008). Halogens and SO_2 may be removed from the atmosphere in solution during water-enhanced sedimentation (known as wet deposition or scrubbing), which is particularly effective in plumes that contain large amounts of external water (e.g. Rose et al. 1995).

Volcanic ash fallout provides a source of nutrients to the oceans and may be an important component of the local ocean-surface iron budget. Transfer of bioaccessible iron from ash particles to surface waters has the potential to stimulate massive phytoplankton blooms and affect nitrogen fixation if fallout occurs in an otherwise productive but iron-poor region of the ocean (high-nutrient, low-chlorophyll conditions) (Duggen et al. 2009). If ash fallout is sustained over months to years and provides sufficiently high iron concentrations, there may be potential for a reduction in atmospheric CO_2 concentration through stimulated biological activity.

ENVIRONMENTAL AND HUMAN IMPACTS

Volcanic ash transports halogens and trace elements to the surface during fallout, which may impact terrestrial ecosystems and human and animal health (Mather et al. 2003). Removal of vapor- and liquid-phase components from volcanic plumes occurs through heterogeneous chemical processes and adsorption onto the surfaces of ash particles, followed by sedimentation through dry and wet deposition (Delmelle et al. 2005). Desorption of chemical compounds from particulates to water transfers a suite of elements and

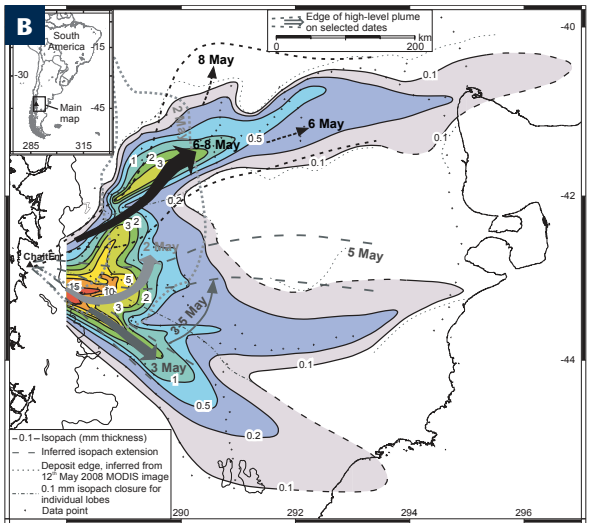

Figure 6 (**A**) Satellite image and (**B**) diagram showing the cloud trajectories (shown by arrows) and the distribution and thickness of the tephra deposit generated by the May 2008 eruptions of Chaitén volcano, Chile. Particulates emitted from a series of eruptions were transported in different directions, which generated a complex deposit over Chile, Argentina and as far east as the Atlantic Ocean (modified from Watt et al. 2009). The satellite image shows the volcanic cloud dispersing southeast over Argentina.

ions that include Cl, Ca, Na, SO_4^{2-}, Mg, and F in a time frame of only minutes (Witham et al. 2005). The presence of fluorine increases fluxes of silicon, phosphorus, and iron (Jones and Gislason 2008).

Ash fallout may cause building collapse due to rapid accumulation and the high density of individual volcanic ash particles (Spence et al. 2005), and can also contaminate water supplies (Stewart et al. 2006). Airborne ash and toxic gases (e.g. SO_2) in high concentrations may present human respiratory health hazards, and there is particular concern about the presence of crystalline silica (e.g. cristobalite) and transition metals such as iron (Fubini and Fenoglio 2007; Horwell and Baxter 2006). On May 2, 2008, Chaitén volcano, Chile, erupted unexpectedly (Fig. 6) (Watt et al. 2009), and ash deposition raised levels of B, Cd, Zn, Tl, Cu, and Ni in aqueous environments and vegetation (Martin et al. 2009). Early fallout included ~2 wt% cristobalite, within which nanofibers were identified for the first time. The cristobalite content rose to 20 wt%, due to vapor-phase crystallization, as a new dome grew (Reich et al. 2009: Horwell et al. 2010). The levels of airborne particulates with a diameter less than 10 µm exceeded safety thresholds in the Argentine town of Esquel (100 km east of Chaitén) for a month after the eruption.

In summary, volcanic emissions impact climate and cloud microphysical processes and chemical reactions, and transfer chemical species to local environments. These emissions disrupt travel and aviation infrastructure at the

Box 1 Properties of Volcanic Particulates

The adjacent figure compares the size ranges of volcanic particles present in volcanic emissions, which consist of a mixture of gases (e.g. H_2O, CO_2, SO_2), aerosol [a dispersion of small (<30 µm) solid or liquid particles in a gas medium, shown in green], and silicate ash particles (particles with a diameter (d) ≤ 2000 µm, shown in blue). The size, shape, and composition of volcanic particles are characterized from samples of airborne or deposited particulates. Aerodynamic and optically based instruments are used to measure the in situ concentration and size characteristics of airborne particulates. Filter samples may also be collected using particle samplers for size and compositional analysis in the laboratory.

Aerosol particle size distributions display four characteristic modes; for details, see Gieré and Querol (2010 this issue).

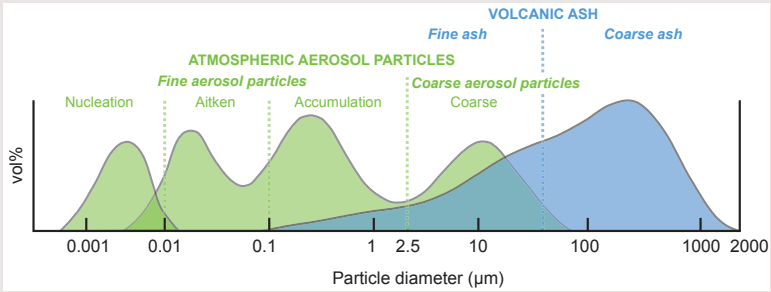

The term *tephra*, Greek for "ashes," describes all fragmented material ejected during explosive volcanic eruption that travels through the atmosphere. Volcanic ash is a subset of tephra and includes silicate particles in the following categories (Cas and Wright 1987): coarse ash (63 µm < d ≤ 2000 µm) and fine ash (d ≤ 63 µm); the size range of fine ash includes the majority of the size classification for coarse and fine aerosol particles. Laser diffraction analysis of particle size is commonly used to give rapid, accurate measurement of ash particles with d less than 2 mm in deposits; coarser samples require the use of size-calibrated sieves. The total weight fraction of volcanic particles with d < 0.1 µm generated in a given eruption is generally negligible.

Volcanic ash includes a dominant "juvenile" component of quenched melt (glass), a "lithic" component of eroded vent wall rock, and a "crystal" component of minerals formed in the magma, which are all liberated during the fragmentation process. Depending on magma composition, the crystal component will consist of different proportions of quartz, feldspar, micas, pyroxenes, amphiboles, and olivine. At dome-forming volcanoes, there may also be significant post-emplacement deposition of vapor-phase crystalline silica (cristobalite, quartz, and tridymite) and feldspar.

surface; these have the potential to generate large economic losses, in addition to impacting human health. More effort should be invested in the measurement of the particle size and mass fraction of fine ash emitted by volcanoes and in the quantification of global ash fluxes to the atmosphere. A complete understanding of the impacts of volcanic particulates will be achieved only through multidisciplinary research strategies involving, for example, field and physical volcanology, atmospheric science, remote sensing, physics, chemistry, biology, and epidemiology.

ACKNOWLEDGMENTS

AJD gratefully acknowledges support from Lockheed Martin Corporation, the European Research Council (DEMONS project), and the UK Natural Environment Research Council. CJH is funded through a NERC Postdoctoral Research Fellowship (NE/C518081/2). The authors thank Fleurice Parat, David Pyle, Martin Reich, Steve Sparks, and two anonymous referees for constructive and helpful reviews that greatly improved this manuscript, and Thomas Jauss for graphical assistance. The authors also express special thanks to Reto Gieré, David Vaughan, and Pierrette Tremblay for editorial assistance and reviews on several versions of the manuscript.

REFERENCES

Bonadonna C, Phillips JC (2003) Sedimentation from strong volcanic plumes. Journal of Geophysical Research 108(B7): 2340, doi:10.1029/2002JB002034

Bonadonna C, Ernst GGJ, Sparks RSJ (1998) Thickness variations and volume estimates of tephra fall deposits; the importance of particle Reynolds number. Journal of Volcanology and Geothermal Research 81: 173-187

Bursik MI, Sparks RSJ, Gilbert JS, Carey SN (1992) Sedimentation of tephra by volcanic plumes: I. Theory and its comparison with a study of the Fogo A plinian deposit, Sao Miguel (Azores). Bulletin of Volcanology 54: 329-344

Cas RAF, Wright JV (1987) Volcanic Successions, Modern and Ancient. Allen & Unwin, London, UK, 528 pp

Deligne NI, Coles SG, Sparks RSJ (2010) Recurrence rates of large explosive volcanic eruptions. Journal of Geophysical Research 115: B06203, doi:10.1029/2009JB006554

Delmelle P, Villiéras F, Pelletier M (2005) Surface area, porosity and water adsorption properties of fine volcanic ash particles. Bulletin of Volcanology 67: 160-169

Duggen S, Olgun N, Croot P, Hoffmann LDH, Teschner C (2009) The role of airborne volcanic ash for the surface ocean biogeochemical iron-cycle: a review. Biogeosciences Discussions 6: 6441-6489

Durant AJ, Shaw RA, Rose WI, Mi Y, Ernst GGJ (2008) Ice nucleation and overseeding of ice in volcanic clouds. Journal of Geophysical Research 113: D09206, doi: 10.1029/2007JD009064

Durant AJ, Rose WI, Sarna-Wojcicki AM, Carey S, Volentik ACM (2009) Hydrometeor-enhanced tephra sedimentation: Constraints from the 18 May 1980 eruption of Mount St. Helens. Journal of Geophysical Research 114: B03204, doi:10.1029/2008JB005756

Fubini B, Fenoglio I (2007) Toxic potential of mineral dusts. Elements 3: 407-414

Gieré R, Querol (2010) Solid particulate matter in the atmosphere. Elements 6: 215-222

Grainger RG, Highwood EJ (2003) Changes in stratospheric composition, chemistry, radiation and climate caused by volcanic eruptions. In: Oppenheimer C, Pyle DM, Barclay J (eds) Volcanic Degassing. Geological Society of London Special Publication 213, London, UK, pp 329-347

Halmer MM, Schmincke H-U, Graf H-F (2002) The annual volcanic gas input into the atmosphere, in particular into the stratosphere: a global data set for the past 100 years. Journal of Volcanology and Geothermal Research 115: 511-528

Horwell CJ, Baxter PJ (2006) The respiratory health hazards of volcanic ash: a review for volcanic risk mitigation. Bulletin of Volcanology 69: 1-24

Horwell CJ, Le Blond JS, Michnowicz SAK, Cressey G (2010) Cristobalite in a rhyolitic lava dome: evolution of ash hazard. Bulletin of Volcanology 72: 249-253

Jones MT, Gislason SR (2008) Rapid releases of metal salts and nutrients following the deposition of volcanic ash into aqueous environments. Geochimica et Cosmochimica Acta 72: 3661-3680

Krueger A, Krotkov N, Carn S (2008) El Chichon: The genesis of volcanic sulfur dioxide monitoring from space. Journal of Volcanology and Geothermal Research 175: 408-414

Lamb HH (1970) Volcanic dust in the atmosphere; with a chronology and assessment of its meteorological significance. Philosophical Transactions of the Royal Society A 266: 425-533

Martin RS, Watt SFL, Pyle DM, Mather TA, Matthews NE, Georg RB, Day JA, Fairhead T, Witt MLI, Quayle BM (2009) Environmental effects of ashfall in Argentina from the 2008 Chaitén volcanic eruption. Journal of Volcanology and Geothermal Research 184: 462-472

Mastin LG and 16 coauthors (2009) A multidisciplinary effort to assign realistic source parameters to models of volcanic ash-cloud transport and dispersion during eruptions. Journal of Volcanology and Geothermal Research 186: 10-21

Mather T, Pyle DM, Oppenheimer C (2003) Tropospheric volcanic aerosol. In: Robock A, Oppenheimer C (eds) Volcanism and the Earth's Atmosphere. American Geophysical Union, pp 189-212

Oppenheimer C (2010) Ultraviolet sensing of volcanic sulfur emissions. Elements 6: 87-92

Prata AJ (2009) Satellite detection of hazardous volcanic clouds and the risk to global air traffic. Natural Hazards 51: 303-324

Pueschel RF, Russell PB, Allen DA, Ferry GV, Snetsinger KG, Livingston JM, Verma S (1994) Physical and optical properties of the Pinatubo volcanic areosol: Aircraft observations with impactors and a Sun-tracking photometer. Journal of Geophysical Research 99: 12915-12922

Pyle DM (2000) Sizes of volcanic eruptions. In: Sigurdsson H, Houghton BF, McNutt SR, Rymer H, Stix J (eds) Encyclopedia of Volcanoes. Academic Press, London, UK, pp 263-269

Pyle DM, Mather TA (2009) Halogens in igneous processes and their fluxes to the atmosphere and oceans from volcanic activity: A review. Chemical Geology 263: 110-121

Reich M, Zúñiga A, Amigo Á, Vargas G, Morata D, Palacios C, Parada MA, Garreaud RD (2009) Formation of cristobalite nanofibers during explosive volcanic eruptions. Geology 37: 435-438

Robock A (2004) Climatic impact of volcanic emissions. In: Robock A, Oppenheimer C (eds) State of the Planet: Frontiers and Challenges in Geophysics. American Geophysical Union, pp 125-134

Rose WI, Delene DJ, Schneider DJ, Bluth GJS, Krueger AJ, Sprod I, McKee C, Davies HL, Ernst GGJ (1995) Ice in the 1994 Rabaul eruption cloud: implications for volcano hazard and atmospheric effects. Nature 375: 477-479

Self S (2006) The effects and consequences of very large explosive volcanic eruptions. Philosophical Transactions of the Royal Society A 364: 2073-2097

Sparks RSJ (1978) The dynamics of bubble formation and growth in magmas: A review and analysis. Journal of Volcanology and Geothermal Research 3: 1-37

Spence RJS, Kelman I, Baxter PJ, Zuccaro G, Petrazzuoli S (2005) Residential building and occupant vulnerability to tephra fall. Natural Hazards and Earth System Sciences 5: 477-494

Stewart C, Johnston DM, Leonard GS, Horwell CJ, Thordarson T, Cronin SJ (2006) Contamination of water supplies by volcanic ashfall: A literature review and simple impact modelling. Journal of Volcanology and Geothermal Research 158: 296-306

Watt SFL, Pyle DM, Mather TA, Martin RS, Matthews NE (2009) Fallout and distribution of volcanic ash over Argentina following the May 2008 explosive eruption of Chaitén, Chile. Journal of Geophysical Research 114: B04207, doi:10.1029/2008JB006219

Witham CS, Oppenheimer C, Horwell CJ (2005) Volcanic ash-leachates: a review and recommendations for sampling methods. Journal of Volcanology and Geothermal Research 141: 299-326